THE FIRST MEASUREMENTS OF CHARON'S FAR-ULTRAVIOLET SURFACE REFLECTANCE. B. A. Keeney[1], J. Wm. Parker[1], N. Cunningham[2], S. A. Stern[1], A. J. Verbiscer[3], and the *New Horizons* Team, [1]Southwest Research Institute, Boulder CO, USA (keeney@boulder.swri.edu), [2]Nebraska Wesleyan University, Lincoln, NE, USA, [3]University of Virginia, Charlottesville, VA, USA.

Introduction: NASA's *New Horizons* mission completed its historic flyby of the Pluto system in July 2015 [1]. Here we present the first measurements of Charon's far-ultraviolet (FUV) surface reflectance, measured by *New Horizons*' Alice ultraviolet spectrograph [2] on approach to the Pluto system.

Charon's mid-ultraviolet (mid-UV) reflectance was previously measured by the *Hubble Space Telescope* [3,4], finding a nearly constant geometric albedo of ≈0.25 from 2250−3300 Å. Its reflectance blueward of 2250 Å could not be measured due to the reduced solar flux at these wavelengths.

Observations: The Alice instrument aboard *New Horizons* is a lightweight, low-power spectrograph with a bandpass of 520−1870 Å [2]. Its imaging microchannel plate detector produces a 1024×32 data array, but only the central 780×21 pixels are illuminated. This study uses the narrow portion of the Alice slit, which covers the bottom two-thirds of the detector. Each detector row subtends 0.3 degrees in the spatial dimension, and the filled-slit spectral resolution is 9 Å.

Alice observations of Charon were obtained as part of longer sequences performed in "ride along" mode where instruments other than Alice dictated spacecraft pointing. We analyze data from four of these sequences taken over a period of 14 hours that ended ~2.5 hours before closest approach. Within each sequence, we focus our analysis on the subset of exposures where Charon's position in the Alice slit is relatively stable.

All exposures were corrected as described in [5] for the effects of detector dead time, dark counts, and scattered light from the wings of the Lyα profile generated by hydrogen in the interplanetary medium. Spectra of Charon were then extracted from individual exposures, and when possible exposures from the same observing sequence were combined using a variance-weighted mean. These coadditions are shown in Figure 1, along with the solar spectrum at Pluto arbitrarily reduced to fit on the scale of the plot. We adopt the solar spectrum of [6], which combines SUMER reference spectra [7] with observations from TIMED/SEE [8] for the *New Horizons* observation dates.

The spectra in Figure 1 are labeled with the name of the observing sequence and the effective exposure time (the amount of time Charon's position was stable in the Alice slit), and the sequences are ordered by decreasing range to Charon. Charon shows no observable flux below 1650 Å in any of the sequences, and the observed flux at longer wavelengths increases as *New Horizons* approaches Charon. However, Charon's position in the Alice slit is most stable (i.e., its effective exposure time is longest) when *New Horizons* is far from Charon. The combination of these effects leads to modest and relatively constant signal-to-noise ratios (3-5 per 1.8-Å pixel) among the sequences.

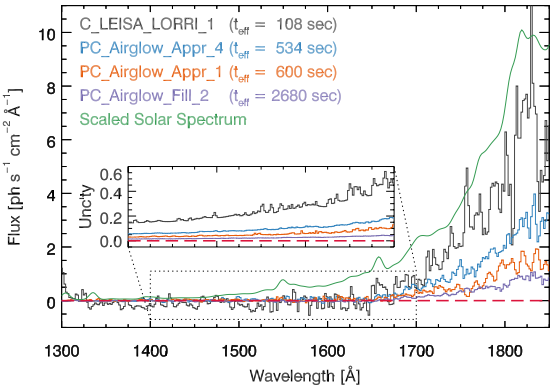

Figure 1: FUV spectra of Charon from Alice observing sequences. A scaled solar spectrum is shown for comparison. The inset shows the 1σ flux uncertainty for each observing sequence from 1400−1700 Å.

Results and Discussion: We determine the radiance of Charon in each observing sequence by dividing the fluxes in Figure 1 by Charon's solid angle as observed by Alice. We then take the ratio of Charon's radiance to the radiance of a Lambertian surface normally illuminated by the Sun (i.e., $F_\odot/\pi$) to derive Charon's surface reflectance (*I/F*). The spectral shape of Charon's *I/F* is the same in all sequences, and the inset of Figure 2 shows the surface reflectance from PC_Airglow_Appr_4 as an example. The characteristic upturn from H_2O ice absorption is present, as the reflectance rapidly increases from zero blueward of 1650 Å to 0.07 at 1725 Å, and remains at that level until 1850 Å.

Solar Phase Dependence. Figure 2 shows Charon's variance-weighted mean *I/F* from 1750–1850 Å as a function of solar phase angle. We estimate two different statistical uncertainties in Charon's surface reflectance. The first is a random uncertainty based on photon-counting (i.e., Poisson) statistics and the second is a systematic uncertainty that accounts for Charon's motion in the Alice slit. We assume a 3%

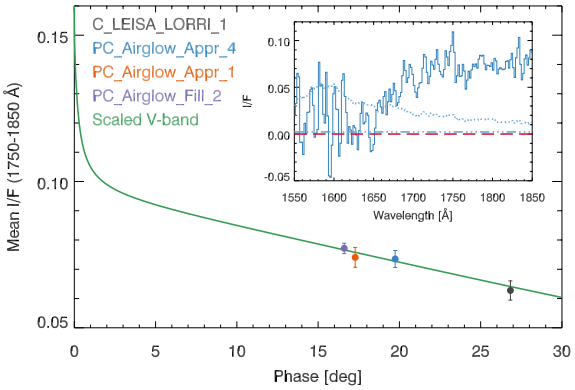

Figure 2: The variance-weighted mean *I/F* of Charon from 1750−1850 Å as a function of solar phase angle. The solid line shows Charon's *V*-band phase curve [9] scaled to match the Alice data. The inset shows the surface reflectance as a function of wavelength for PC_Airglow_Appr_4. The dotted line shows the 1σ random uncertainty in *I/F* and the dot-dashed line shows the 1σ systematic uncertainty.

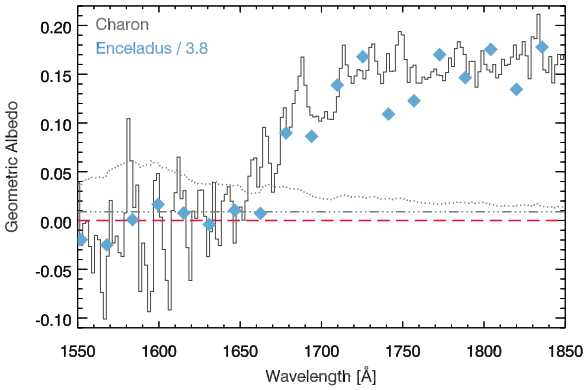

Figure 3: The geometric albedo as a function of wavelength for Charon (black line) and Enceladus (blue diamonds; [10]). The dotted line shows the 1σ random uncertainty and the dot-dashed line shows the 1σ systematic uncertainty in Charon's geometric albedo. When the geometric albedo of Enceladus is reduced by a factor of 3.8 it is very similar to Charon's.

systematic pointing uncertainty for sequences where Charon fills the slit, and a 1% pointing uncertainty for sequences where it does not, since Charon's position in the Alice slit was never perfectly stable because other instruments dictated spacecraft pointing. Further, for sequences where Charon scans through the Alice slit we assume a 2-s uncertainty on the effective exposure time because its precise value is somewhat subjective.

Since Charon's *I/F* is nearly constant at these wavelengths (see inset) and we are averaging over >50 pixels, the random uncertainties in the mean *I/F* are quite small despite the modest signal-to-noise ratio of the data; however, the systematic uncertainties are not reduced when averaging. The error bars in Figure 2 are the quadrature sum of the random and systematic uncertainties for each sequence.

We use the photometric model of [9] to study changes in Charon's relative FUV reflectance with solar phase. This model is fit to *V*-band images of Charon from *Hubble* and *New Horizons* spanning solar phase angles of <0.01−170 degrees. A least-squares fit finds that the solar phase curve of [9] matches the Alice data when a multiplicative scale factor of 0.3760±0.0065 is applied, as was done to produce the solid line in Figure 2.

Charon's FUV Geometric Albedo. Since the scaled *V*-band solar phase curve of [9] is a good match to the Alice data, we use it to correct the sequences to zero phase to determine Charon's FUV geometric albedo. We combine all sequences using a variance-weighted mean to increase the signal-to-noise ratio. Figure 3 shows the geometric albedo of Charon obtained from averaging all of the Alice observing sequences.

Charon's geometric albedo at 1800 Å (0.16±0.01) is significantly lower than the value of ≈0.25 from 2250−3000 Å found by [3,4], and the FUV spectral slope is not large enough to reconcile the measurements. However, this difference is not surprising since Charon is composed primarily of H_2O ice, like the saturnian satellites, and H_2O-ice-rich surfaces decrease strongly in reflectance between 2250 Å and 1850 Å [10].

Figure 3 compares the geometric albedo of Charon as a function of wavelength to that of Enceladus using Cassini/UVIS data from [10]. After reducing the geometric albedo of Enceladus by a factor of 3.8, we find that they have very similar spectral shapes in the FUV since both their surfaces are primarily H_2O ice.

Acknowledgments: This work was supported by NASA's *New Horizons* project.

References: [1] Stern, S. A., Bagenal, F., Ennico, K., et al. (2015) *Science*, 350, aad1815. [2] Stern, S. A., Slater, D. C., Scherrer, J., et al. (2008) *Space Sci. Rev.*, 140, 155. [3] Krasnopolsky, V. A. (2001) *Icarus*, 153, 277. [4] Stern, S. A., Cunningham, N. J., Hain, M. J., Spencer, J. R., & Shinn, A. (2012) *Astron. J.*, 143, 22. [5] Steffl, A. J., Young, L. A., Strobel, D. F., et al. (2020) *Astron. J.*, 159, 274. [6] Young, L. A., Kammer, J. A., Steffl, A. J., et al. (2018) *Icarus*, 300, 174. [7] Curdt, W., Brekke, P., Feldman, U., et al. (2001) *Astron. & Astroph.*, 375, 591. [8] Woods, T. N., Eparvier, F. G., Bailey, S. M., et al. (2005) *JGR (Space Phys.)*, 110, A01312. [9] Howett, C. J. A., Olkin, C. B., Protopapa, S., et al. (2021) in *The Pluto System After New Horizons*, ed. S. A. Stern, R. P. Binzel, W. M. Grundy, J. M. Moore, & L. A. Young (Univ. of Arizona Press). [10] Hendrix, A. R., Filacchione, G., Paranicas, C., Schenk, P., & Scipioni, F. (2018) *Icarus*, 300, 103.